AIP | Review of Scientific Instruments

An acoustic resonance measurement cell for liquid property determinations up to 250°C

Blake T. Sturtevant, Cristian Pantea, and Dipen N. Sinha

Citation: Rev. Sci. Instrum. **83**, 115106 (2012); doi: 10.1063/1.4765746
View online: http://dx.doi.org/10.1063/1.4765746
View Table of Contents: http://rsi.aip.org/resource/1/RSINAK/v83/i11
Published by the American Institute of Physics.

An acoustic resonance measurement cell for liquid property determinations up to 250 °C

Blake T. Sturtevant,[a] Cristian Pantea, and Dipen N. Sinha
Los Alamos National Laboratory, Materials Physics and Applications, Los Alamos, New Mexico 87544, USA

(Received 6 September 2012; accepted 21 October 2012; published online 27 November 2012)

This paper reports on the development of a compact, rugged, and portable measurement cell design for the determination of liquid sound speed at temperatures up to 250 °C and pressures up to 3000 psi. Although a significant amount of work exists in the literature on the characterization of fluids, primarily pure water, over a wide range of pressures and temperatures, the availability of experimentally determined sound speed in water between 100 °C and 250 °C is very limited. The need to measure sound speed in liquids up to 250 °C is of both fundamental interest, as in the case of basic equations of state, and applied interest, such as for characterizing geothermal or petroleum downhole environments. The measurement cell reported here represents an advancement in the established room temperature swept frequency acoustic interferometry measurement for liquid sound speed determinations. The paper details the selection of materials suitable for high temperature operation and the construction of the measurement apparatus. Representative sound speeds as a function of temperature and pressure are presented and are shown to be in very good agreement with an internationally accepted standard for water sound speed. © *2012 American Institute of Physics*. [http://dx.doi.org/10.1063/1.4765746]

I. INTRODUCTION

The measurement of sound speed in a fluid as a function of both temperature and pressure is very useful for the determination of accurate equations of state. To this end, many works have reported on instruments for performing measurements of sound speed in liquids as a function of these two state variables.[1–12] The range of pressures for which liquid water sound speeds have been reported, up to 3.5 GPa, is significantly more comprehensive than the range of temperatures studied which is largely up to 100 °C.[4–9,12–14] Most of the sound speed measuring instruments reported in the literature are complex custom-made instruments requiring high-precision machining and fabrication. Additionally, previous instruments tend to be non-portable and largely inseparable from the test environment; the sample is introduced into the instrument rather than the instrument being moveable from one test environment to another. A summary of the evolution of laboratory-based velocimeters can be found in Ref. 15.

There are many applications requiring a device for measuring liquid sound speed that is capable of performing high precision measurements, is portable between test environments, is mechanically rugged, and is able to withstand high temperatures. An example of such an application is for the characterization of enhanced geothermal systems (EGS) or hot dry rock (HDR) working fluids. More than 97% of the United States' land area at depths up to 10 km are at temperatures of 250 °C or lower,[16] making this temperature an ideal target for characterization instruments. While the high pressures of downhole environments can be accommodated by incorporating appropriately thick walls in the device packaging, the temperatures characteristic of downhole applications are more difficult to address from a materials compatibility standpoint and serve as the motivation for the present work. In addition to high temperature challenges, the fluids in geothermal systems are chemically harsh brines which are very corrosive, particularly at high temperatures. Sound speed varies with many physical parameters of a liquid such as temperature, pressure, and dissolved solid or gas content.[15] Thus, when used with complimentary characterization tools, sound speed provides valuable information regarding the dynamics of a fluid system. We report here on the development of an acoustic resonance cell for sound speed measurements that is capable of performing at this elevated temperature, is mechanically rugged, and offers a precision better than 0.1%. This measurement cell has been repeatedly used at temperatures up to 250 °C and pressures up to 3000 psig.

The high temperature-high pressure measurement cell reported here is based on swept frequency acoustic interferometry (SFAI), an established technique for fluid characterization at room temperature that is capable of achieving high precision in sound speed determinations.[17] In the SFAI technique, the acoustic resonances of a fluid-filled cavity are measured over a range of frequencies and provide information from which the fluid sound speed, attenuation, and density can be determined.[17] The present work is concerned with only the determination of sound speed. Historically, SFAI resonant cavities have been delicate instruments, being constructed of high purity, optically polished glass and being excited with commercially available broadband transducers whose operation is limited to the vicinity of room temperature. In constructing a high temperature and high pressure SFAI (HTP-SFAI) measurement cell capable of operation at 250 °C, the primary challenges were faced in the identification of materials that were capable of operating at higher temperatures. These challenges and their solutions are addressed below.

[a]Author to whom correspondence should be addressed. Electronic mail: bsturtev@lanl.gov.

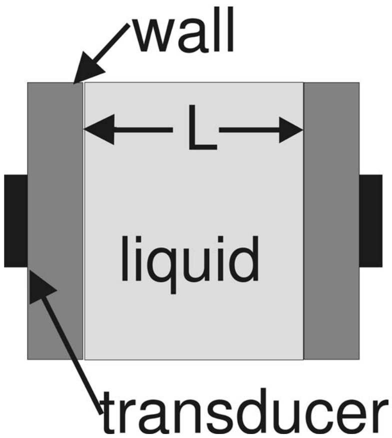

FIG. 1. Simplified schematic of a SFAI cell. The liquid occupies the resonant cavity of length L which is bounded by two parallel walls. Piezoelectric transducers are used to input and extract energy from the system.

After a brief overview of the SFAI theory in Sec. II, the details of the cell construction are described in Sec. III. For illustrative purposes, example data sets collected as a function of temperature and pressure are provided in Sec. IV and are compared to accepted values for the sound speed of water calculated using Ref. 18. Finally, Sec. V concludes the paper.

II. OVERVIEW OF SFAI THEORY

At the core of a SFAI experimental setup is a fluid-filled acoustic resonant cavity with piezoelectric transducers that are used to input and extract energy from the system as shown schematically in Fig. 1.[17] Using an appropriate electronic setup, such as a vector network analyzer, the frequency response of the transducer/wall/fluid-filled cavity system can be obtained. An example of a transmission spectrum is shown in Fig. 2. The resonant frequencies, where transmission is maximized, can be identified from such a spectrum. Resonances are observed when forward and backward traveling acoustic waves interfere constructively. This interference leads to standing waves and occurs when the liquid path length, L, is an integer number of half wavelengths of the wave: $\lambda_n = 2L/n$ where n is an integer indicating the harmonic number. Using the wave relation $c = f_n\lambda_n$, the resonant frequencies, f_n, can be expressed in terms of the path length and the sound speed in the liquid, c_L: $f_n = nc_L/2L$. Measurement of L and at least two f_n thus enables determination of the sound speed

$$c_L = 2L\frac{df_n}{dn}, \tag{1}$$

where df_n/dn measures the frequency spacing between successive higher order harmonics (n, $n+1$, $n+2$, ...). In principle, two f_n are sufficient to determine $df_n/dn = f_{n+1} - f_n$. However, greater precision in df_n/dn can be achieved by considering a larger number of f_n.

In practice, SFAI cells do not consist solely of single fluid layers; the walls and transducers each have their respective resonant frequencies. At frequencies around the wall or transducer resonances, energy is coupled between the wall or transducer and the fluid. This energy coupling serves to decrease the spacing between fluid resonance peaks and affects the accurate determination of df_n/dn.[17] For this reason, these regions are avoided when selecting fluid peaks for calculating df_n/dn. The transducer, wall and liquid resonances can be seen in Fig. 2. The transducers have a resonance frequency at ~5 MHz, the wall resonance frequencies are spaced at roughly 800 kHz (shown with a gray envelope in Fig. 2), and the desired fluid resonances are spaced at roughly 80 kHz.

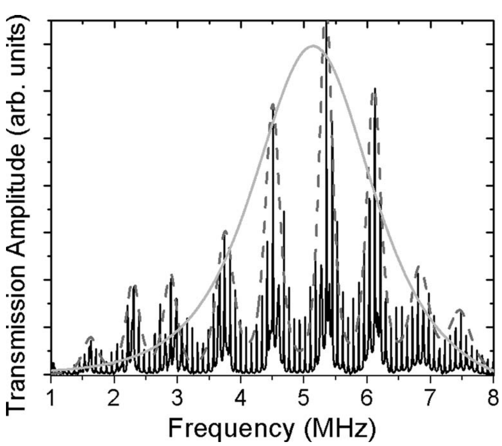

FIG. 2. A typical SFAI spectrum. Three sets of resonances can be seen. The resonance of the 5 MHz lithium niobate transducers dominates the overall power spectrum of the measurement cell as indicated with the solid gray trace. The SFAI cavity walls have their own resonances with ~800 kHz spacing, shown by the dashed gray envelope. Finally, the fluid resonant peaks, spaced at ~80 kHz, are seen throughout the entire spectrum.

III. EXPERIMENTAL SETUP

A. Measurement cell details

This section describes the materials used and the procedure of constructing a SFAI cell for use in high temperature and/or high pressure environments. The piezoelectric elements of the measurement cell (the "transducers" in Fig. 1) consist of two lithium niobate ($LiNbO_3$) crystals with 5 MHz fundamental frequencies (Boston PiezoOptics, Inc., Bellingham, MA). Lithium niobate was chosen over common alternatives because it has significantly higher piezoelectric coupling than quartz and, with a Curie temperature of 1210 °C,[19,20] is operable at significantly higher temperatures than lead zirconium titanate (PZT). The 36° Y-rotated cut of lithium niobate having "Z-Y′-Z″ convention"[21] Euler angles (90°, −36°, 0°) was chosen because it excites a pure-longitudinal acoustic mode. No shear component was desired since the cell is used to study fluids. The 10 mm diameter crystals were metalized with Cr/Au in a standard coaxial configuration and had an active area 7 mm in diameter.[22]

To protect the transducers from mechanically and chemically harsh test environments, a stainless steel package was constructed using commercially available Swagelok and Conflat (CF) fittings. A well was bored in 1-1/3″ CF blank flange to accommodate a single lithium niobate transducer (see Fig. 3(a)). The well had a diameter of 12.5 mm, a depth of 3.2 mm, and a bottom surface that was smooth and parallel to the front face of the flange to within 25 μm. Most gels that are commonly used to acoustically couple piezoelectric

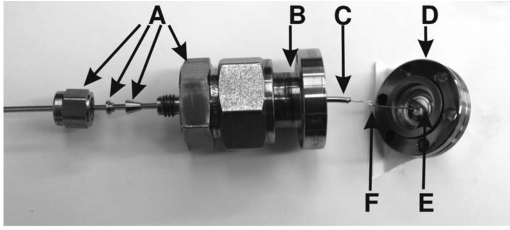

(a)

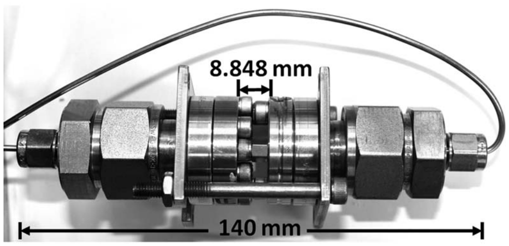

(b)

FIG. 3. (a) The construction of a packaged high temperature and pressure acoustic transducer including a 2 mm-0.75″ Swagelok union (A), 1-1/3″ Conflat half-nipple (B), high temperature stainless steel sheathed coaxial cable (C), 1-1/3″ Conflat blank flange with a custom well 3.2 mm deep × 12.5 mm in diameter bored out (D), a 5 MHz 36° Y-rotated lithium niobate transducer (E), and a flexible Kapton insulated wire (F) for making the connection between the coax center conductor and the transducer. (b) Two packaged transducers arranged opposing each other for transmission mode SFAI measurements. The length, L = 8.848 mm, of the resonant cavity is defined by the bolt heads with spacers used to hold the CF flange together. The measurement cell is compact at 14 cm in length.

transducers to other components of a system are water-based and thus unsuitable for use at the target temperature of 250 °C. For the HTP-SFAI cell, a number of high temperature organic and ceramic-based adhesives were tested to acoustically couple the transducer to the CF flange with differing degrees of success. Some of the adhesives tested formed voids due to outgassing during the curing process, which significantly degrades the ability to transmit ultrasound. Other adhesives had coefficients of thermal expansion that were drastically different than that of the transducers and caused excessive stress, sometimes resulting in destruction of the transducer, at higher temperatures. Ultimately, the best acoustic couplant in terms of high temperature stability and efficiency of ultrasound transmission was a commercially available specialty high temperature epoxy (Epoxy H24 from Epoxy Technologies, Inc., Billerica, MA). The CF blank is mated to a 1-1/3″ half nipple and sealed using a copper gasket capable of withstanding >250 °C. The half nipple is connected to a 0.75″ to 2 mm Swagelok reducing union as shown in Fig. 3(a). The 2 mm end of the Swagelok reducing union accommodates a high temperature (∼600 °C) stainless steel-sheathed coaxial cable (Thermocoax, Inc.) that is used to transmit the signal to and from the cell. The stainless steel sheath of the coaxial cable protects the copper center conductor from mechanical or chemical damage while the mineral powder dielectric allows this cable to be used well above the 250 °C temperature required for this application. Because the coaxial cable is rigid, a flexible Katpon insulated wire was used to connect the coax center conductor to the transducer. The flexibility of this wire allows the Swagelok and Conflat assembly to be sealed after all electrical connections have been made. Electrical connections between the coaxial cable and the transducer were made using a high temperature silver-filled epoxy (E4110-LV, also from Epoxy Technology, Inc.). This epoxy was chosen because it was found to maintain a low resistivity and showed little degradation in preliminary furnace tests up to 400 °C. Two of the stainless steel packaged transducers shown in Fig. 3(a) were arranged facing each other (Fig. 3(b)) with the front faces of the CF blanks defining the boundaries of the SFAI cell. On one transducer package, the CF blank flange was fastened to the CF half nipple using six standard 3/4″ long bolts. On the other transducer package, the CF blank flange was fastened using three 3/4″ long bolts and three bolts which included an additional spacer, one of which can be seen in Fig. 3(b). The three bolts with the additional spacers define the physical dimension of the resonant cavity, L.

B. Test environment

A pressure vessel rated to 500 °C and 5000 PSI (model# 4681, Parr Instrument Company, Moline, IL) was used as a test environment for demonstrating the measurement cell. The 1 l volume of the pressure vessel was filled with 700 ml of distilled, degassed water. The measurement cell itself occupies a volume of ∼100 ml and the remaining ∼200 ml headspace consisted of nominally whole air. The signal-carrying coaxial cables were sealed to the pressure vessel using Grafoil gland compression fittings (MHM2 series, Conax Technologies, Buffalo, NY). The pressure vessel is fitted with a furnace heater and temperature controller. The internal pressure can be controlled independently of temperature by pressurizing the headspace in the vessel. Because a freshly filled gas cylinder can provide a maximum pressure of ∼2300 psi, a pressure amplifier with a 30:1 piston head area ratio (Model: AAD-30, Haskel International, Inc., Burbank, CA) was used to enable repeated testing up to 3000 psig. An 80 psig house air source was used to drive the amplifier and a compressed N_2 cylinder provided the working gas at a pressure of ∼1000 psig on the low pressure side of the regulator. The maximum pressure of 3000 psig used for testing represents a constraint imposed by the test environment and not of the measurement cell itself. The temperature inside the water test fluid was monitored with an accuracy of ±1.1 °C and a precision of ±0.1 °C using a type-J thermocouple (Model M8MJSS-M2-U-250, Omega Engineering, Inc.). The system pressure was measured to an accuracy of ±13 psi using a pressure transducer with a 0-5000 psig range (Model PX309-5KG5V, Omega Engineering, Inc.). To collect the data presented below, a vector network analyzer (Model Bode 100, Omicron electronics Corp., Houston, TX) was used to measure the S_{21} forward transmission scattering parameter.

IV. EXAMPLE DATA AND ANALYSIS

This section first shows how a liquid sound speed can be determined from an $|S_{21}|$ transmission spectrum and then presents two representative sets of liquid water speeds, first as

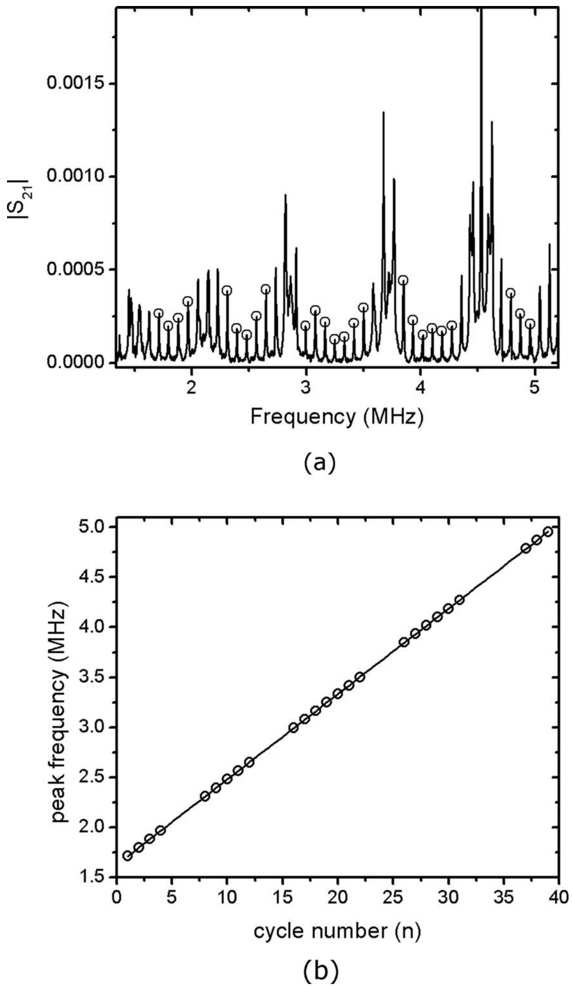

FIG. 4. (a) The center frequency of 25 f_n, indicated with open circles, in regions not affected by wall or transducer resonances, were selected for calculation of df_n/dn. (b) These center frequencies plotted vs n, with skipped cycles accounted for and a linear fit shown.

a function of pressure and also along the liquid-vapor coexistence line where both temperature and pressure vary.

A. Determining sound speed from $|S_{21}|$ spectrum

Figure 4(a) shows a representative plot of the transmission scattering parameter, $|S_{21}|$, vs. frequency, collected at 30 °C and ambient pressure. Many fluid resonance peaks can be identified from such a plot. Twenty-five of these resonances, chosen because they are apart from wall and transducer resonances as described in Sec. II, are indicated with circles in the figure. To determine df_n/dn, the frequencies of the resonances identified in Fig. 4(a) are plotted against "cycle number" while taking care to account for cycles for which resonances are not recorded (specifically: n = [5-7, 13-15, 22-25, 32-36]) as shown in Fig. 4(b). For the purpose of determining sound speed, it is only necessary to know n in a relative and not an absolute sense since the slope of f_n vs n is the only quantity of interest. A linear least-squares fit, shown in Fig. 4(b), can be performed on the data to determine df_n/dn. For the 25 resonances shown in Fig. 4, a least-squares fit determined $\frac{df_n}{dn} = 85.408 \pm 0.033$ kHz. Using a measured path length, L = 8.848 mm, the sound speed is determined to be 1511.4 ± 0.6 m/s. The standard deviation, $\sigma = 33$ Hz, of the linear fit slope is reported as the uncertainty here. This uncertainty contributes to a relative uncertainty in sound speed of 0.04%.

TABLE I. Comparison of experimentally determined and predicted sound speed.

Temp (°C)	Pressure (psig)	Determined sound speed (m/s)	Predicted sound speed (m/s), Ref. 18
30.4	7	1511.8	1512.0
30.4	195	1513.7	1514.0
30.5	397	1516.1	1516.3
30.4	600	1518.4	1518.5
30.5	797	1521.0	1520.9
30.6	999	1523.0	1523.4
30.6	1205	1525.4	1525.6
30.7	1400	1528.1	1528.0
30.7	1606	1530.2	1530.3
30.8	1798	1532.9	1532.7
30.9	1997	1534.8	1535.1
31	2195	1537.2	1537.6
31.2	2402	1540.1	1540.4
31.3	2602	1543.0	1542.8
31.4	2813	1544.9	1545.4
31.4	2995	1547.2	1547.5

B. Sound speed as a function of pressure at 31 °C

The first set of data presented here was collected at 30.9 ± 0.5 °C at 20 pressures between ambient pressure and 3000 psig. Table I presents the determined sound speed vs. pressure data along with the sound speed calculated by the IAPWS-IF97 standard.[18] The IAPWS-IF97 sound speeds are not experimental points, but are calculated from the equation of state for water given in Ref. 18. The equations used in these calculations are found in Ref. 18 while the full set of experimental thermodynamic data upon which the equation of state is based are described in Ref. 22. The IAPWS calculations are used for comparison since there is no previous single set of direct sound speed measurements over the entire temperature and pressure range reported here. To determine the sound speed from a measured transmission spectrum, df_n/dn was calculated as described in Sec. IV A. The path length, L = 8.848 mm, was calibrated using deionized and degassed 25 °C water as a standard. As a result of the test environment described in Sec. III B, pressure changes were accompanied by small changes in temperature due to compression or expansion of the gas in the headspace of the vessel. Because an increase in temperature of 1 °C has the same effect on the sound speed in water as increasing the pressure by 200 psi, the slightly different temperatures had to be accounted for when comparing measurements against predicted values. In all cases, the determined sound speeds agree with the IAPWS-IF97 values to within 0.5 m/s. This agreement provides a validation for the measurement precision determined by the linear fit of f_n vs n.

TABLE II. Experimentally determined and predicted water sound speeds along the liquid-vapor coexistence curve.

Temperature (°C)	Determined sound speed (m/s)	Predicted sound speed (m/s), Ref. 18	Difference[a] (%)
27.5	1504.4	1504.7	− 0.02
30.3	1510.2	1511.5	− 0.09
45.5	1538.5	1539.6	− 0.07
56.5	1548.7	1551.3	− 0.17
57.3	1549.9	1551.9	− 0.13
70.4	1555.2	1557.5	− 0.15
84.5	1555.0	1555.5	− 0.03
90.3	1551.1	1552.5	− 0.09
104.8	1539.1	1540.3	− 0.08
109.6	1534.3	1534.9	− 0.04
120.5	1518.0	1520.3	− 0.15
132.1	1500.6	1501.3	− 0.05
141.4	1483.4	1483.9	− 0.03
151.4	1462.1	1462.9	− 0.05
163.1	1436.0	1435.7	0.03
171.6	1412.9	1414.1	− 0.09
184.4	1378.7	1378.8	− 0.01
199.8	1331.1	1332.1	− 0.08
210.1	1297.1	1298.3	− 0.10
223.1	1252.8	1252.8	0.00
235.6	1206.2	1206.0	0.01
250.4	1143.6	1146.7	− 0.28

[a]Difference = 100* (measured−calculated)/measured.

C. Liquid water sound speeds measured along the liquid-vapor coexistence curve

The second set of data presented here was collected in liquid water at 22 temperatures between laboratory ambient and 250 °C at pressures corresponding to the liquid-vapor coexistence line. At each temperature, the sound speed was determined using the procedure described above. The path length, L, was corrected for changes in temperature using a calibrated 25 °C value of L and a linear thermal coefficient of expansion for stainless steel of 16×10^{-6}/°C. The measured data show very good agreement with the IAPWS-IF97 predicted sound speeds[18] as can be seen from Fig. 5 and Table II. For all points, the discrepancy between the measured and IAPWS-IF97 predicted sound speed is better than 0.3% (∼3 m/s). The discrepancies are likely attributed to errors in the temperature measurements by the thermocouple. At higher temperatures especially, a small error in temperature can have a significant impact on the sound speed of water. For example, at 220 °C, a change in temperature of 1 °C leads to a 3.6 m/s change in water sound speed. The inability to measure temperature to better than about 1 °C reflects limitations of the present test environment and does not affect the measurement precision of the HTP-SFAI measurement cell. As indicated above and in Table I, the precision of the measurement cell is better estimated by the standard deviation in df_n/dn and is typically in the range of 0.5 m/s or better.

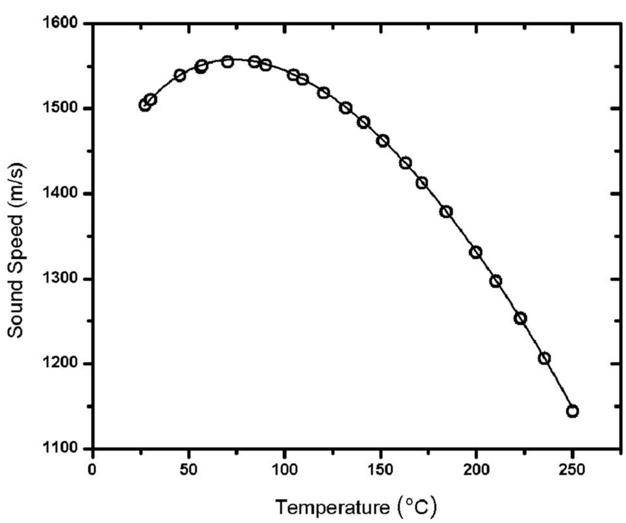

FIG. 5. The speed of sound in water up to 250.4 °C along the liquid-vapor coexistence curve. The 22 open circles represent sound speeds determined from SFAI measurements while the solid trace corresponds to sound speeds calculated from Ref. 18 . The values are provided in Table II.

V. CONCLUSIONS

This paper reports a new measurement cell that can be used for resonance-based sound speed measurements in fluids up to temperatures of 250 °C and pressures of at least 3000 psig. The measurement cell is based on the room temperature swept frequency acoustic interferometry technique but advances the state-of-the-art by using commercially available specialty adhesives and a simply constructed stainless steel housing to equip it for immersion in thermally, mechanically, and chemically harsh environments.

Example sound speed data as a function of temperature and pressure were presented as a demonstration of the measurement cell capabilities. The data were compared to the internationally accepted standard, IAPWS-IF97, and shown to be in very good agreement at temperatures up to 250 °C and pressures up to 3000 psig. The precision achieved with the measurement cell is shown to be significantly better than 0.1%.

ACKNOWLEDGMENTS

This work was supported by the (U.S.) Department of Energy (DOE) under Award No. AID 18832.

[1]R. T. Beyer, J. Acoust. Soc. Am. **32**(6), 719–721 (1960).
[2]C. T. Chen, R. A. Fine, and F. J. Millero, J. Chem. Phys. **66**(5), 2142–2144 (1977).
[3]J. R. Davies, J. Tapson, and B. J. P. Mortimer, Ultrasonics **38**(1-8), 284–291 (2000).
[4]V. Del Grosso, J. Acoust. Soc. Am. **47**(3), 947 (1970).
[5]W. M. Madigosky, I. Rosenbaum, and R. Lucas, J. Acoust. Soc. Am. **69**(6), 1639–1643 (1981).
[6]K. Meier and S. Kabelac, Rev. Sci. Instrum. **77**(12), 123903 (2006).
[7]F. Plantier, J. L. Daridon, and B. Lagourette, J. Acoust. Soc. Am. **111**(2), 707–715 (2002).
[8]S. Vance and J. M. Brown, J. Acoust. Soc. Am. **127**(1), 174–180 (2010).
[9]W. D. Wilson, J. Acoust. Soc. Am. **31**(8), 1067–1072 (1959).
[10]Z. Zhu, M. S. Roos, W. N. Cobb, and K. Jensen, J. Acoust. Soc. Am. **74**(5), 1518–1521 (1983).
[11]G. Holton, M. P. Hagelberg, S. Kao, and W. H. Johnson, J. Acoust. Soc. Am. **43**(1), 102 (1968).
[12]S. Wiryana, L. J. Slutsky, and J. M. Brown, Earth Planet. Sci. Lett. **163**(1-4), 123–130 (1998).

[13]A. A. Aleksandrov and A. I. Kochetov, Therm. Eng. **26**(9), 558–559 (1979).
[14]K. Fujii and R. Masui, J. Acoust. Soc. Am. **93**(1), 276–282 (1993).
[15]C. C. Leroy, in *Elastic Properties of Fluids: Liquids and Gases*, edited by D. S. Moises Levy and R. Raspet (Academic, New York, 2001), Vol. 4.
[16]J. W. Tester, B. J. Anderson, A. S. Batchelor, D. D. Blackwell, R. D. E. M. Drake, J. Garnish, B. Livesay, M. C. Moore, K. Nichols, S. Petty, M. N. Toksoz, and J. R. W. Veatch, *The Future of Geothermal Energy: Impact of Enhanced Geothermal Systems (EGS) on the United States in the 21st Century* (Massachusetts Institute of Technology, 2006).
[17]D. N. Sinha and G. Kaduchak, in *Experimental Methods in the Physical Sciences*, edited by H. E. B. Moises Levy and S. Richard (Academic, 2001), Vol. 39, pp. 307–333.
[18]W. Wagner and H.-J. Kretzschmar, *International Steam Tables: Properties of Water and Steam Based on the Industrial Formulation IAPWS-IF97*, 2nd ed. (Springer-Verlag, Berlin, 2008).
[19]B. J. James, in *Proceedings of the 42nd Annual Frequency Control Symposium 1988*, IEEE Catalog No. 88CH2588-2 (IEEE, 1988), pp. 146–154.
[20]A. W. Warner, M. Onoe, and G. A. Coquin, J. Acoust. Soc. Am. **42**(6), 1223 (1967).
[21]B. A. Auld, *Acoustic Fields and Waves in Solids* (Krieger, 1990).
[22]W. Wagner and A. Pruss, J. Phys. Chem. Ref. Data **31**(2), 387–535 (2002).